Hyperfine Interactions **132:** 245–254, 2001.
© 2001 *Kluwer Academic Publishers. Printed in the Netherlands.*

The SPEG Mass Measurement Program at GANIL

H. SAVAJOLS
GANIL, BP 5027, 14076 Caen cedex 05, France

Abstract. The measurement of masses (or binding energy) of nuclei far from stability is of fundamental interest for our understanding of nuclear structure. Their knowledge over a broad range of the nuclear chart is an excellent and severe test of nuclear models. This is why considerable experimental and theoretical efforts have been and are invested in this domain. Here we want to give a description of direct mass measurements combining high-resolution time-of-flight determinations and accurate momentum measurements in a spectrometer. This very fast and direct method was developed at GANIL with the high-resolution spectrometer SPEG. The mass measurements realised and scheduled provide important first indications of new regions of deformation or shell closures very far from stability.

Key words: atomic mass, nuclear binding energy, mass spectrometer, time-of-flight.

1. Introduction

The precision required in a mass measurement is highly variable. In some applications the binding energy must be known with a precision of a keV or better (QED, QCD). Very far from stability, the mass predictions diverge to the level of MeV. Hence measurements at this level of accuracy or somewhat better, of the order of 100 keV, will provide significant constraints. Nonetheless, direct mass measurements corresponding to a determination of the binding energy with an error of 100 keV need a high resolution and a high precision. Indeed, for a nucleus of mass $A = 100$, a precision of the order of $1 \cdot 10^{-6}$ is necessary. By a time-of-flight method this level of accuracy requires a relatively long flight path ($\sim$100 m) to a high resolution spectrometer. The SPEG technique has no significant lifetime limitation and can be employed with very low secondary beam intensities (0.01 particle/s). Therefore mass measurements of very exotic nuclei, located close to the drip-line in the mass region of $A \sim 10$–40, are accessible.

The following discussion is divided into four main parts: (a) the production of exotic nuclei far from stability for mass measurements, (b) the SPEG method, (c) some results, and (d) the future of the SPEG mass measurement program.

2. Production of nuclei far from stability

At GANIL, nuclei far from stability are produced following the reaction of an intense heavy ion beam (10^{13} pps) at intermediate energy (50–100 A MeV), on a

production target. The dominant mechanism in this energy domain is the fragmentation of the projectile. The projectile like fragments are then selected in flight by the beam line α-shaped spectrometer and transported to the high-resolution spectrometer SPEG [1]. The energy of the fragments are of the order of a few GeV. The power of this process for the production of exotic nuclei stems essentially from the concentration of the cross section within a very small angular and velocity range as the incident beam energy increases. This production mechanism is well suited for achieve a high transmission in a spectrometer, that may at the same time provide the selection of nuclei of interest. Predictions of cross-section are incorporated in codes, such as LISE [2] or as INTENSITY [3], which include selection by a magnetic spectrometer. Such codes are very useful for preparing an experiment, to define the most suited reaction and the magnetic and eventually electric parameters of the spectrometer.

Typically, projectile fragmentation of $^{40-48}$Ca and ^{64}Ni has been used to measure masses of very neutron-rich nuclei. The fragmentation of a ^{78}Kr beam was used to measure masses of proton-rich nuclei near the $N = Z$ line.

To increase the transmitted yield of exotic nuclei, a dedicated device called SISSI [4] has been constructed. It consists of a set of two superconducting solenoid lenses of very short focal length (0.6 m). The first solenoid is used to focus the incoming beam in a spot of ± 0.2 mm on a fast rotating target. The second provides an increase in the transport line angular acceptance. A large acceptance angle of up to ± 80 mrad is achieved with a small emittance of 16π mm mrad due to the small beam spot. This allows to transport the secondary beam with a standard beam line.

In order to have a broad range of reference masses which is a crucial point in a direct mass measurement, the production target rotating at around 2000 turns/min in the SISSI device has steps of different thickness. In the last mass measurement the tantalum target was divided in three parts, i.e., 89% has a thickness of 550 mg/cm^2 for the nuclei of interest and 10 and 1% has a thickness of 450 mg/cm^2 and 250 mg/cm^2 to produce heavy reference masses with suitable count rates.

3. Experimental procedure

The method used is a direct time-of-flight technique (Figure 1). The power of this approach comes from the coupling of the projectile fragmentation as a production method to the high-resolution spectrometer SPEG. The very broad elemental and isotopic distributions resulting from such reactions combined with the fast in-flight electromagnetic selection can provide the mapping of an entire region of the nuclear mass surface in a single measurement.

The beam line from the exit of the α-spectrometer and the focal plane of the SPEG spectrometer is doubly achromatic. In such a device, the mass is deduced from the relation

$$B\rho = \frac{\gamma m_0 v}{q},$$

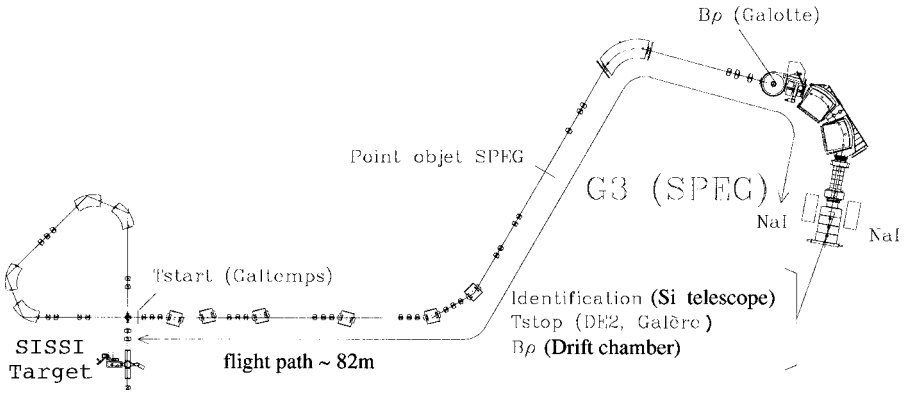

Figure 1. Experimental set-up.

where B_ρ is the magnetic rigidity of a particle of a rest mass m_0, charge q and velocity v and γ the Lorentz factor. This technique requires only a precise determination of the magnetic rigidity and the velocity of the ion.

The time-of-flight (ToF) is measured using a pair of microchannel plate detector systems located near the production target (start signal) and at the final focal plane of SPEG (stop signal). The flight times are typically of the order of 1 μs for a path 82 m long. The intrinsic resolution of the start and stop detectors are of the order of 100–200 ps (FWHM) leading to a time-of-flight resolution of $\Delta t/t \sim 2 \cdot 10^{-4}$. One crucial problem in direct mass measurements is to eliminate systematic errors in the time-of-flight determination due to differential nonlinearities of the electronic chains, i.e., time-to-amplitude and analog-to-digital converters. For that purpose, we use time signals from a precise high-frequency clock uncorrelated with the beam. The period used is $TC = 80$ ns. Time differences from such signals and both start and stop signals are measured for each nucleus. These time differences are random, and differential nonlinearities are then averaged over the whole range of TACs and ADCs. According to this technique, determination of the time-of-flight follows the relation

$$T_{\text{vol}} = T_{\text{start}} - T_{\text{stop}} + N \cdot TC + T_0,$$

where T_{start} and T_{stop} are the time differences, N is the number of TC periods and T_0 is a constant.

The magnetic rigidity δ of each ion is derived from two horizontal position measurements. The first measurement is performed by a thin position-sensitive microchannel plate system located at the dispersive image planes of the analysing magnet, i.e., at the conventional target chamber where the dispersion in momentum is big (10 cm/%). The second is made by two drift chambers used after the spectrometer. Thus reconstruction trajectories of each ion is possible and we accurately determine the value of the magnetic rigidity independantly of the object size. A momentum resolution of 10^{-4} is commonly achieved.

The identification of each ion arriving at the focal plane of SPEG is achieved by the measured flight time and the energy loss and total energy signals from a detector telescope. The telescope consists of four cooled silicon detectors of typical ticknesses of 50, 300, 6000 and 6000 μm. The energy loss signal is obtained by summing the signals from the first two elements of the telescope, while the total energy signal is obtained by summing all first three detectors. The last silicon detector is used in anticoincidence.

A number of points should be considered carefully. The population of isomeric states with lifetimes of the order or greater than the flight time through the system ($\sim$1μs) is a potential problem, as the resolution of the system is not sufficient to resolve the typical mass difference between the ground and isomeric excited states. The contribution of such states will lead to a systematic shift in the measurement towards less bound masses. For ^{32}Al an isomeric state in a ratio of about 2% has been found [8]. As a check that the deduced masses are not affected by the existence of isomers, the device includes the detection of delayed γ-rays by a 4π NaI array surrounding the telescope.

A mass resolution of $2\text{–}4 \cdot 10^{-4}$ is obtained from the combination of the time-of-flight and the magnetic rigidity measurement. This corresponds to ± 3 MeV of the mass excess, for a nucleus $A = 40$ the final uncertainties range from 100 keV for thousands of events (nuclei relatively close to stability) to 1 MeV for tens of events (nuclei approaching the ends of isotopic chains).

As noted above, a large number of nuclei ($\sim$100) are transmitted in a single setting of the beam line and the spectrometer (Figure 2). The nuclei with well-known masses and with adequate yield provide a calibration from which the unknown masses are derived. Such a large number of reference masses over a wide range of Z and A is particularly important for providing final mass determinations with precisions of the order of 10^{-6}. In the last mass measurement experiment [24], only masses where three or more independant and compatible mass determinations were available were used as references.

From these references we estimate in each case the systematic uncertainty introduced by the method. A mass is then deduced from an interpolation done by a Taylor series between the references. The terms of this series reflect the small inaccuracies (or adjustments) in the method. A typical development for the mass determination is

$$m_0 = Z\left(\alpha_1(1+\delta)T_{\text{vol}}\gamma^{-1} + \alpha_2\right) + \alpha_3 A + \alpha_4 Z + \alpha_5 M^2 + \alpha_6 \frac{M^3}{Z^2},$$

where the first four terms could be considered as a first order adjustment. The last two terms are higher order corrections. The fifth term corresponds to the difference in the time collection of ions in the silicon telescope. The last term corresponds to effects related to energy loss of particles in the emisive foils of microchannel plate detectors or entrance foils of both small drift chambers. The constants α_1–α_6 are adjusted for known nuclei. Mass uncertainties include statistical, calibration and

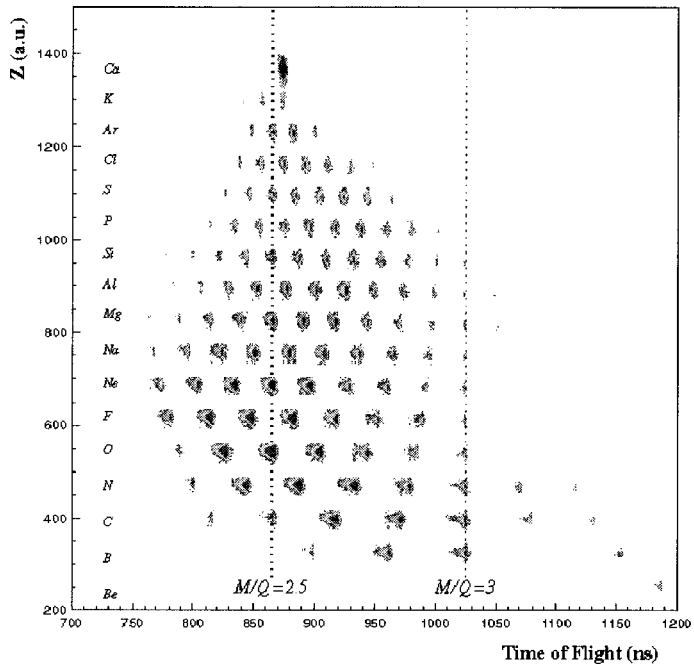

Figure 2. Transmitted nuclei, identification matrix Z vs. time-of-flight (ToF).

extrapolation errors. Of course the farther away the extrapolation, the bigger is the extrapolation error.

4. Results of mass measurements

The first mass measurement with SPEG took place in 1986. Since then many experiments have been performed in the region of light and medium nuclei. Indeed, the limit for obtaining reasonable mass determinations with present detector technology is $A \sim 80$.

On the proton-rich side, the fragmentation of a ^{78}Kr beam on a Ni target has been used to reach nuclei near the $N = Z$ line in the mass region $A \sim 60$–80 SPEG98 [5]. These masses are important for providing input for astrophysical modelling for the rp process and for information on the nuclear structure in a region of high deformation. As more than 200 nuclides are produced in this fragmentation reaction, with high yields for nuclei close to the stability, it was necessary to purify the secondary beams. The method is based on the stripping of the ions in a thin foil located the two dipole stages of the α-spectrometer. It allows the selection in terms of atomic number Z, and does not increase beam emittance. The mass excesses of ^{70}Se and ^{71}Se have been determined with a precision of $\sim 5.10^{-6}$ [5]. These results agree well with the estimates of Audi and Wapstra based on systematic trends.

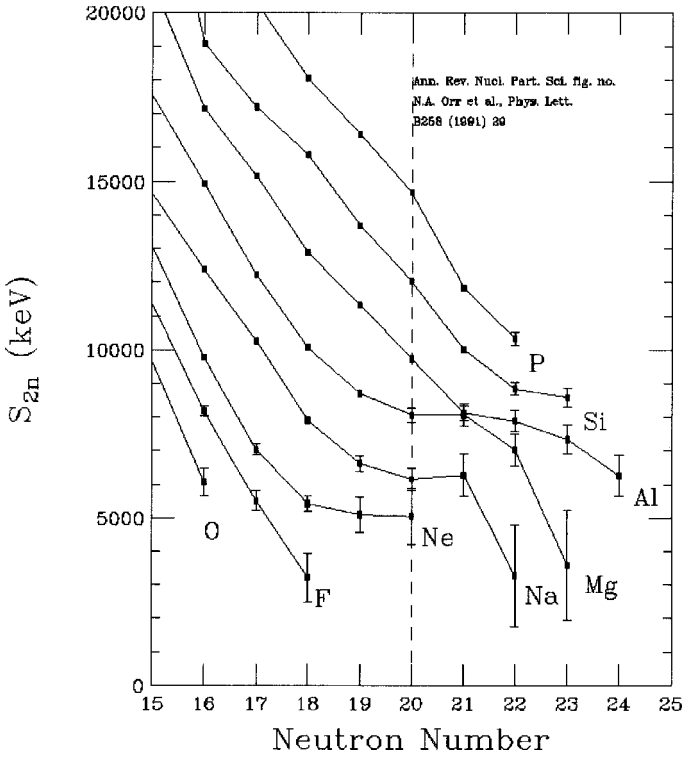

Figure 3. Two neutron separation energy S_{2n} as a function of the neutron number N for neutron-rich nuclei in the vicinity of the $N = 20$ shell closure.

On the neutron-rich side, efforts were made to measure masses near the $N = 20$ and $N = 28$ shell. Indeed, the evolution of shell closures far from stability is a subject of much actual debate. Deformations, shape coexistence or variations in the spin orbit strength as a function of the neutron to proton ratio could provoke the modification of magic numbers. The more natural observable that may probe this change in the standard shell ordering is the separation energy of the last two neutrons, S_{2n}.

Around $N = 20$, two groups using different time-of-flight recoil spectrometers, the TOFI [6] and the SPEG systems, dedicated mass measurements in that region. Figure 3 shows the S_{2n}-values as a function of the neutron number in the vicinity of the $N = 20$ shell closure collected in the SPEG86 [7], SPEG87 [8] and SPEG91 [9] campains. The results of Ne, Na and Mg isotopes exhibit an anomaly around $N = 20$. An overbinding, corresponding to an increase in the two neutron separation energies, at the neutron sd-shell closure is observed, where a decrease would be expected. Additionally, a much lower than expected excitation energy was determined for the first 2^+ state in ^{32}Mg [10, 11]. This overbinding is related by the breaking of the $N = 20$ magicity where an island of deformation is observed. These results have been confirmed by Coulomb excitation [20] and theoretical

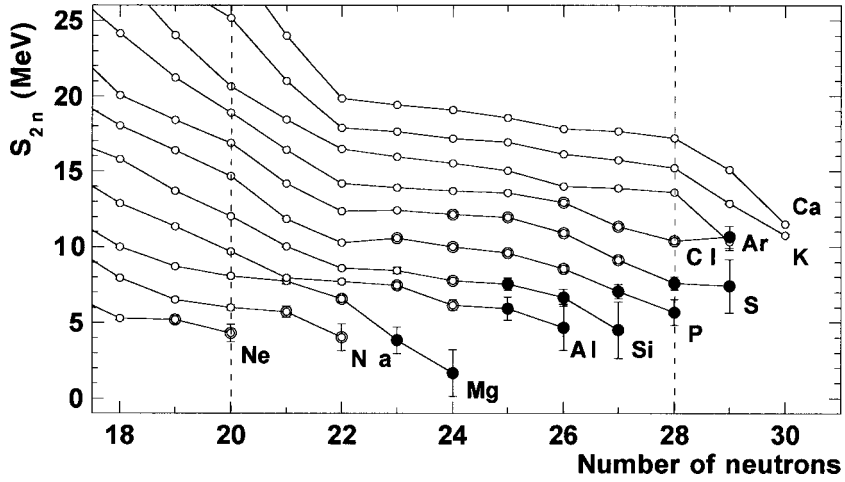

Figure 4. Experimental S_{2n} values in the region of the $N = 20$ and $N = 28$ shell closures. The circles correspond to values from [25], the bold circles to values for which the precision was improved and the full circles to masses measured for the first time.

calculations [13–19]. It is commonly accepted that this island of deformation is due to the mixing with the next shell, the deformed intruder $f_{7/2}$.

More recently, the determination of the lifetime and of the deformation of ^{44}S showed indications of a similar effect [22, 23] at $N = 28$. These were the motivations for a mass measurement experiment (SPEG99 [24]) to investigate the $N = 28$ shell closures for nuclei from Si ($Z = 14$) to Ar ($Z = 18$). The production of these neutron-rich nuclei has been obtained by the fragmentation of a ^{48}Ca beam at 60 A MeV on a Ta target located in the SISSI device. Data we obtained and the recently published [25] mass determinations allowed us to reanalyse unpublished experimental results from SPEG91 [26], where the lack of reference masses did not allow masses to be extracted for nuclei heavier than $A = 37$. Masses of 31 neutron-rich nuclei have been measured in the vicinity of $N = 20$ and $N = 28$ gaps. As can be seen on Figure 4, the precision for 19 masses was improved, often by about a factor 2 or more. Twelve masses were measured for the first time, 8 of them with a precision of better than 1 MeV. The Ca isotopes show the typical behavior of the filling of shells with the two shell closures at $N = 20$ and $N = 28$ (decrease of the S_{2n} at $N = 20$, and a slowly decreasing in S_{2n} as the $1f_{7/2}$ shell is filled). The K and Ar isotopes show a similar behavior. The Cl, S and P isotopes however, exhibit a pronounced change of slope around $N = 26$.

Since the S_{2n} values correspond to a derivative of the mass surface, a more direct way to see shell effects on nuclear masses is to substract the macroscopic contribution. Here we have used the finite range liquid drop model (FRLDM) [27] and have defined the shell correction as

$$\text{Shell correction} = dM_{\text{exp}} - dM_{\text{FRLDM}},$$

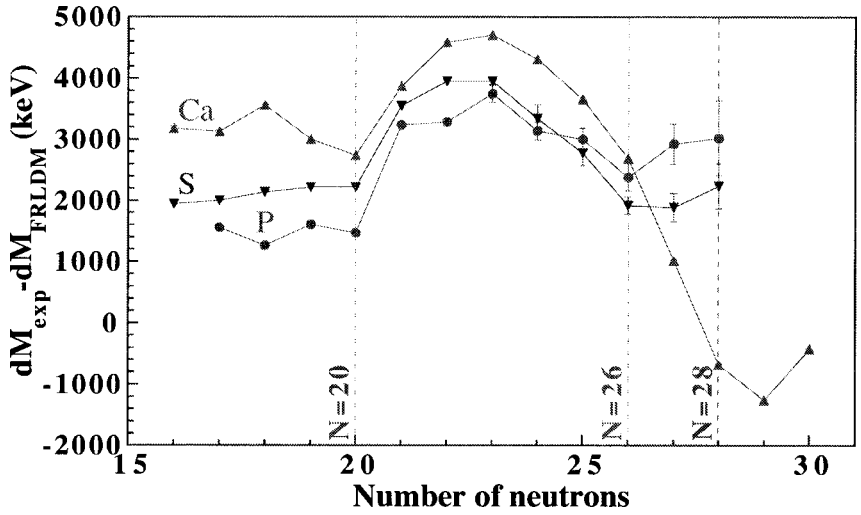

Figure 5. Shell correction as defined in the text of the mass Ca, S and P.

where dM_{exp} is the experimental mass excess and dM_{FRLDM} is the macroscopic part of the FRLDM. The shell correction energy is plotted in Figure 5. As in Figure 4, the qualitatively different behavior of the S and P isotopes as compared to the Ca isotopes is clearly evident. The Ca isotopes show pronounced shell correction minima around $N = 20$ and $N = 28$. The S and P isotopes do not exhibit such effects at $N = 28$, and show a discontinuity in the slope at $N = 26$.

From experimental masses, two different independant observables, the S_{2n}-values and shell correction, show the same behavior. These results are reproduced by shell model [19] and relativistic mean field calculations [28]. The models predict that deformed prolate ground state configurations associated with shape coexistence are necessary to explain the experimental data. The existence of an isomeric state in the ^{43}S in the same experiment and its interpretation by shell model calculations confirm the analysis of the masses and constitutes the first evidence of shape coexistence in this region [29].

5. Future and perspectives

For both $N = 20$ and $N = 28$ shell gap studies far from stability, mass measurements with SPEG have brought clear evidence on a change in the shell structure. This behavior is mainly associated with gain of binding energy through the deformation which would have consequences to the drip line location.

A new measurement to extend mass beyond the $N = 20$ shell gap is scheduled for the beginning of 2001 [30]. As can be seen in Figure 4, new results have been obtained too, for Ne to Al isotopes. In particular, the steep decrease of the S_{2n}-values for Mg may imply that the Mg isotopes may become unbound with respect to two neutron emissions for a much lower neutron number than the predicted

value of $N \geqslant 28$ in models [20, 31, 32]. The set-up will be optimized to get a large amount of $^{36-37}$Mg as well as $^{30-32}$Ne. In this new experiment we also hope to be able to extend our mass measurement around $N = 28$ for the Al, Si and P isotopes (pseudo $N = 26$ shell closure) and get new mass data for lighter nuclei located at the border of the drip-line (pseudo $N = 16$ shell closure) when going from O to F isotopes.

A first improvement with respect to previous measurements will be an increase of the current of the primary ^{48}Ca beam, to at least an intensity of 7 eμA (instead of 600 enA). To be able to work with the highest possible beam currents and transmission we plan to use a thin degrador in the beam line α-spectrometer. This wedge will help to remove light particles which were one of the beam intensity limitations in the SPEG99 experiment. We will have to prove that this does not introduce uncontrolled systematic errors.

A second improvement concerns the time-of-flight resolution. Recent developments (we initiated) concerning a new design of microchannel plate detectors give us an intrinsic resolution of the order of 70 ps (FWHM), i.e., a gain of a factor ∼3. Another promising way is to use a "chemical vapour deposition" (CVD) diamond detector [33]. A time resolution below 50 ps (σ) and a single particle count rate capability of 10^8 ion/s are achieved with this type of heavy-ion detectors [34]. We could use this material as degrader and as a start signal in the beam line spectrometer. Therefore, we will gain about 20 m in the path length and improve our time-of-flight resolution.

6. Summary

The direct time-of-flight method with SPEG is one of the important advances in the last decade for the measurement of masses far from stability. The technique has no lifetime limitation and can be used with very low event rates. Therefore, this is at present the only method for measuring masses up to the neutron drip-line in the mass region $A \sim$10–50. The masses thus obtained provide a means of identifying new nuclear structure effects that are well illustrated by our work in the $N = 20$ and $N = 28$ region. Further studies of a more detailed and experimentally complex nature, such as Coulomb excitation and decay spectroscopy, may then be performed on selected nuclei.

Improvements in the technique, which are still possible, will give us a unique opportunity to measure masses for nuclei at the limit of stability. The measurement of nuclear binding energies far from stability provides an early stimulus for the development of nuclear models.

Acknowledgements

I am grateful to Wolfgang Mittig, who has initiated the mass measurement program with SPEG, and to all people who collaborated in SPEG experiments (see [5, 7–9, 24]).

References

1. Bianchi, L. *et al.*, *Nuclear Instrum. Methods A* **276** (1989), 509.
2. Tarasov, O. *et al.*, `http://www.ganil.fr/lise/proglise.html`.
3. Winger, J. *et al.*, *Nuclear Instrum. Methods B* **70** (1992), 380.
4. Joubert, A., *IEEE* **1** (1991).
5. Chartier, M. *et al.*, *Nuclear Phys. A* **637** (1998), 3.
6. Wouters, J. M. *et al.*, *Nuclear Instrum. Methods A* **240** (1985), 77.
7. Gillibert, A. *et al.*, *Phys. Lett. B* **176** (1986), 317.
8. Gillibert, A. *et al.*, *Phys. Lett. B* **192** (1987), 39.
9. Orr, N. A. *et al.*, *Phys. Lett. B* **258** (1991), 29.
10. Detraz, C. *et al.*, *Phys. Rev. C* **19** (1979), 164.
11. Guillermaud-Mueller, D. *et al.*, *Nuclear Phys. A* **426** (1984), 3.
12. Motobayashi, T. *et al.*, *Phys. Lett. B* **346** (1995), 9.
13. Campi, X. *et al.*, *Nuclear Phys. A* **251** (1975), 193.
14. Wildenthal, B. H. *et al.*, *Phys. Rev. C* **28** (1983), 1343.
15. Poves, A. *et al.*, *Nuclear Phys. A* **571** (1994), 221.
16. Warburton, E. K. *et al.*, *Phys. Rev. C* **41** (1990), 1147.
17. Werner,T. R. *et al.*, *Phys. Lett. B* **335** (1994), 259; *Nuclear Phys. A* **597** (1996), 327.
18. Retamosa, J. *et al.*, *Phys. Rev. C* **55** (1997), 1266.
19. Caurrier, E. *et al.*, *Phys. Rev. C* **58** (1998), 2033.
20. Ren, Z. *et al.*, *Phys. Lett. B* **380** (1996), 241.
21. Pfeiffer, B. *et al.*, *Z. Phys. A* **357** (1997), 235.
22. Sorlin, O. *et al.*, *Phys. Rev. C* **47** (1993), 2941.
23. Glasmacher, T. *et al.*, *Phys. Lett. B* **395** (1997), 163.
24. Sarazin, F. *et al.*, *Phys. Rev. Lett.* **84** (2000), 5062.
25. Audi, G. *et al.*, *Nuclear Phys. A* **624** (1997), 1.
26. Orr, N. A. and Mittig, W., unpublished.
27. Moller, P. and Nix, J. R., *At. Data Nucl. Data Tables* **59** (1995), 185.
28. Ren, Z., RMF code, informations on request.
29. Sarazin, F. *et al.*, In: *APAC'2000 Proceedings*.
30. Savajols, H., E364 GANIL proposal.
31. Haustein, P. E. (ed.), *At. Data Nucl. Data Tables* **39** (1988), 185.
32. Utsuno, Y. *et al.*, to be published.
33. Tapper, R. J., *Rep. Progr. Phys.* **63** (2000), 1273.
34. Berdermann, E. *et al.*, preprint 2000-09 GSI.